HERA-B - note/05-015
HERA-B - Physics/05-012

J/ψ production cross section at $\sqrt{s} = 41.6$ GeV by means of NRQCD calculations

M. Bargiotti[1], A. Bertin[1], M. Bruschi[1], S. De Castro[1], L. Fabbri[1], P. Faccioli[1], B. Giacobbe[1], F. Grimaldi[1], F. Maltoni[2], I. Massa[1], M. Piccinini[1], N. Semprini-Cesari[1], J. Spengler[3], R. Spighi[1], M. Villa[1], A. Vitale[1], A. Zoccoli[1]

[1]*Dipartimento di Fisica dell' Università di Bologna and INFN Sezione di Bologna, I-40126 Bologna, Italy*
[2]*Institut de Physique Théorique, Université Catholique de Louvain Chemin du Cyclotron, 2, B-1348 Louvain-la-Neuve, Belgium*
[3]*Max-Planck-Institut für Kernphysik, D-69117 Heidelberg, Germany* [1]

Abstract

In this note we describe an analysis performed on the existing data on charmonium hadroproduction based on NRQCD calculations. All the existing data on J/ψ and $\psi(2S)$ production in fixed-target experiments and on pp collisions at low energy have been updated. The data have been fitted following a NRQCD approach by studying the color-octet contributions in the charmonium production. This analysis provided the following J/ψ and $\psi(2S)$ production cross section at $\sqrt{s} = 41.6$ GeV: $\sigma_{J/\psi} = (502 \pm 44)$ nb/nucleon, $\sigma_{\psi(2S)} = (65 \pm 11)$ nb/nucleon and $R_\psi = \sigma_{\psi(2S)}/\sigma_{J/\psi} = (0.130 \pm 0.019)$. Detailed studies have been carried out in order to determine the systematic uncertainties on these results.

1 Introduction

The production of charmonium and bottomonium states at high-energy collisions has always been the subject of considerable interest. From the experimental point of view, charmonium decays into lepton pairs offer very clean signatures that are used not only for triggering and calibration but also to perform important physics studies. The decay $B \to J/\psi + X$, for instance, provides an easy handle to QCD studies of b production and to the precise determination of some of the CKM parameters, such as $\sin\beta$. It will be widely exploited also at the LHC, one application being the momentum measurements of B-mesons in $t\bar{t}$ events which allow a very precise top mass determination.

The importance of quarkonium is widely recognized also by the theoretical community. Charmonium and bottomonium states offer a unique laboratory for testing our understanding of QCD, and in particular of the interplay between the perturbative and non-perturbative regimes, which describe the physics of heavy-quark creation and that of bound state formation, respectively. The so-called color-singlet

[1]supported by the Bundesministerium für Bildung und Forschung, FRG, under contract numbers 05-7MP25I

model [1, 2] has been superseded by a rigorous framework, based on the use of non-relativistic QCD (NRQCD) [3], an effective field theory that consistently includes relativistic corrections and provides a solid ground for accurate theoretical analyses.

However, despite the theoretical developments and successes, not all the predictions of the NRQCD factorization approach have been firmly established. The first example is the universality of the non-pertubative matrix elements, on which the predictive power of this approach relies. However, measurements at the Tevatron in proton-proton collisions suggest larger values for the color-octet matrix elements than those obtained at HERA in electron-proton collisions [4]. Even more problematic is the measurement of J/ψ polarization at the Tevatron. NRQCD predicts a sizable transverse polarization for J/ψ's at high-p_T, in contrast with the latest data that now clearly indicate that J/ψ's are produced unpolarized [5]. While there is no quantitative and accepted explanation for this behaviour, it is generally argued that because the quarkonium mass is still not very large with respect to the QCD scale, in particular for the charmonium system, non-factorizable corrections may not be suppressed enough and/or the expansions in NRQCD may not converge very well.

In the light of the present uncertain status, detailed studies on the range of applicability of the NRQCD approach, above all for charmonium states, are certainly welcome. In this work, we perform the NRQCD analysis of all fixed-target experimental data on charmonium production, with the exclusion of that induced by pion beams. Our purpose is threefold. First we present an up-to-date collection of the experimental data on charmonium production in fixed-target experiments. Second we study whether data are consistent with the NRQCD approach and in particular we extract information on the color-octet contributions, to be compared with that obtained from other experiments. Finally we obtain the J/ψ and $\psi(2S)$ cross sections at the HERA-B cms-energy. These values will be used for normalization in other HERA-B analyses. Our analysis is similar to the one presented in Ref. [6], improving on it both in the accuracy of the theoretical predictions and in the treatment of the experimental data. The outline of the paper is as follows. In the following section, we briefly review the framework of the NRQCD approach and state the theoretical results and assumptions that go into our predictions. In Section 3 we collect the experimental data. In Section 4 we describe the strategy used for the fit and in Section 5 we present and discuss the results.

2 The NRQCD approach

In the NRQCD approach, the cross section for producing a quarkonium state H in a nucleon-nucleon interaction can be expressed as a sum of terms, each of which factors into a short-distance coefficient and a long-distance matrix element:

$$\sigma(pp \to H + X) = \sum_{i,j} \int dx_1 dx_2 f_{i/p} f_{j/p} \sum_n \hat{\sigma}(ij \to Q\overline{Q}\,[n] + x)\, \langle \mathcal{O}^H\,[n] \rangle, \tag{1}$$

where i, j are partons and n denotes the color, spin and angular momentum state of an intermediate $Q\overline{Q}$ pair. The short-distance cross section $\hat{\sigma}$ can be calculated perturbatively in the strong coupling α_s. The NRQCD matrix elements $\langle \mathcal{O}^H[n] \rangle$ (see Ref. [3] for their definition) are related to the non-perturbative transition probabilities from the $Q\overline{Q}$ state n into the quarkonium H. They scale with a definite power of the intrinsic heavy-quark velocity v ($v^2 \sim 0.3$ for charmonium and $v^2 \sim 0.1$ for bottomonium) [7]. The general expression (1) is thus a double expansion in powers of α_s and v. While a formal and general proof of Eq.(1) is still lacking, it has been recently shown [8] that it holds for high-p_T quarkonium production up to two loops. In this work, we simply assume that soft effects do not spoil factorization and Eq.(1) holds true also for total cross sections.

H	$\langle \mathcal{O}_1^H \rangle$	$\langle \mathcal{O}_8^H[^3S_1] \rangle$	$\langle \mathcal{O}_8^H[^1S_0^{(8)}] \rangle = \langle \mathcal{O}_8[^3P_0^{(8)}] \rangle / m_c^2$
J/ψ	1.16 GeV^3	$1.19 \cdot 10^{-2}$ GeV^3	$1.0 \cdot 10^{-2}$ GeV^3
$\psi(2S)$	0.76 GeV^3	$0.50 \cdot 10^{-2}$ GeV^3	$0.42 \cdot 10^{-2}$ GeV^3
χ_0	0.11 GeV^5	$0.31 \cdot 10^{-2}$ GeV^3	

Table 1: Reference NRQCD matrix elements for charmonium production. The color-singlet matrix elements are taken from the potential model calculation of [12, 13]. The color-octet matrix elements have been extracted from the CDF data [14] in Ref. [15].

The color-singlet short distance coefficients for spin singlet S-wave ($^1S_0^{[1]}$), P-waves and all the leading color-octet coefficients are known at NLO both for photon-proton and proton-proton collisions [9, 10]. The color-singlet coefficient for $^3S_1^{[1]}$ is known at NLO only for photon-proton collisions [11]. In this respect our analysis cannot be considered as fully at NLO and should be updated once the NLO calculation for the color singlet term will be available. On the other hand, this is not an important limitation to our results, as it will be made clear in the following.

The non-perturbative matrix elements have to be extracted from the data. For the color-singlet terms this is straightforward. It can be easily shown that up to relativistic corrections of order v^4, they can be related to those appearing in the corresponding decay rates and therefore can be extracted from measurements of decay widths. On the other hand, color-octet matrix elements can be only extracted from production processes, such as photoproduction or hadroproduction. The factorization hypothesis implies that the values extracted from different experiments should be universal. Tab. 1 shows the results of a fit performed on the CDF charmonium data [14], for the leading color octet terms involved in $J/\psi, \psi(2S)$ and χ_{cj} production at the Tevatron [15]. For S-waves the fact that transverse momentum distributions coming from CP-even states ($^1S_0^{[8]}$ and $^3P_J^{[8]}$) and the $^3S_1^{[8]}$ have different shapes, has been exploited to obtain information on their relative size. Such a detailed information is not available in fixed-target experiments, where normally only results on total production rates are given.

The analysis performed here is based on a code implementing the NLO calculations of Ref. [10]. For the theoretical inputs, we make the following choices. We use $\mu_0 = 2m_c$ with $m_c = 1.5$ GeV as our central value for the renormalization, factorization and NRQCD scales (all taken equal). We estimate the associated uncertainty by varying the scales between μ_0 and $4\mu_0$. The strong coupling, $\alpha_S(m_Z)$ is tuned to the one used by the PDF sets, *i.e.*, CTEQ6m [16] and MRST2002nlo [17]. We exploit spin symmetry to reduce the number of independent non-perturbative matrix elements,

$$\begin{aligned} \langle \mathcal{O}_8^{\psi}(^3P_J) \rangle &= (2J+1)\, \langle \mathcal{O}_8^{\psi}(^3P_0) \rangle \\ \langle \mathcal{O}_8^{\chi_{cJ}}(^3S_1) \rangle &= (2J+1)\, \langle \mathcal{O}_8^{\chi_{c0}}(^3S_1) \rangle \\ \langle \mathcal{O}_1^{\chi_{cJ}}(^3P_J) \rangle &= (2J+1)\, \langle \mathcal{O}_1^{\chi_{c0}}(^3P_0) \rangle \end{aligned} \qquad (2)$$

and consider only leading color octet corrections. We take the non-perturbative matrix elements collected in Tab. 1 as our reference values. [2] Color-singlet matrix elements are kept fixed. For the color-octet

[2] See also Ref. [18] for a more recent analysis.

matrix elements we adopt the relative normalization as that obtained from the Tevatron data, but for the S-wave color-octet matrix-element two overall multiplicative numbers $\lambda_{J/\psi}$ and $\lambda_{\psi(2S)}$ are introduced to be fitted with the fixed-target data. $\langle \mathcal{O}_8^{\chi c0}(^3S_1)\rangle$ is left fixed to the reference value extracted from the Tevatron. With the above assumptions, the data are fitted with only two free parameters, the λ's, which can be interpreted as the fractions of the "overall Tevatron octet contribution" for J/ψ and $\psi(2S)$ necessary to explain the fixed-target data.

The following theoretical expressions for the cross sections are used

$$\begin{aligned}
&\sigma_{\psi(2S)} = \sigma^{\rm D}_{\psi(2S)},\\
&\sigma_{J/\psi} = \sigma^{\rm D}_{J/\psi} + \sum_{j=0}^{2} {\rm Br}(\chi_{jc} \to J/\psi\gamma)\, \sigma^{\rm D}_{\chi_c} + {\rm Br}(\psi(2S) \to J/\psi X)\, \sigma_{\psi(2S)},\\
&R_\psi = \frac{\sigma_{\psi(2S)}}{\sigma_{J/\psi}},
\end{aligned} \tag{3}$$

where the superscript D refers to the direct contribution. We also define the fraction of J/ψ's coming from χ_{cj} decays as

$$R_\chi \;=\; \frac{\sigma_\chi(J/\psi)}{\sigma_{J/\psi}}, \tag{4}$$

where

$$\sigma_\chi(J/\psi) = \sum_{j=0}^{2} {\rm Br}(\chi_{jc} \to J/\psi\gamma)\, \left[\sigma^{\rm D}_{\chi_c} + {\rm Br}(\psi(2S) \to \chi_{jc}X)\sigma^{\rm D}_{\psi(2S)}\right]. \tag{5}$$

R_χ is an interesting quantity to measure since many uncertainties are expected to cancel in ratios of cross sections. For the branching ratio we use [19]

$$\begin{aligned}
{\rm Br}(\psi(2S) \to J/\psi X) &= 57.6\%,\\
{\rm Br}(\chi_{0c} \to J/\psi\gamma) &= 1.18\%,\\
{\rm Br}(\chi_{1c} \to J/\psi\gamma) &= 31.6\%,\\
{\rm Br}(\chi_{2c} \to J/\psi\gamma) &= 20.2\%.
\end{aligned} \tag{6}$$

3 Present experimental situation

The measurements of J/ψ hadroproduction have been performed in a time period spanning about 30 years. Over such a long period, several different experimental techniques have been used and different input information was available at the time of the measurements. Therefore, comparing results of different experiments on an equal footing requires an update of the published numbers for several aspects. For example, the charmonium branching ratios have changed with time and the treatment of the nuclear effects are not homogeneous. In our compilations, we begin by updating all the measurements with the current best knowledge of branching ratios and nuclear effects.

3.1 Compilation of J/ψ cross sections

The cross section for J/ψ production on a nuclear target of mass number A is parametrized as

$$\sigma^{J/\psi}_{pA} = \sigma_{J/\psi} \cdot A^\alpha. \tag{7}$$

The results collected in Table 2 are rescaled and updated in the following way:

- The actual branching fractions [19] (5.88±0.10% for $J/\psi \to \mu^+\mu^-$ and 5.93±0.10% for $J/\psi \to e^+e^-$) are applied.
- The target mass dependence is taken into account by using the most precise measurement of $\alpha = 0.96 \pm 0.01$ [20] at $x_F(J/\psi)$ =0, with the assumption of its independence on the cms-energy.
- When the forward cross section ($x_F(J/\psi) > 0$) is given, we multiply it by 2 to obtain the total cross section (assumption of symmetric $d\sigma_{J/\psi}/dx_F$ distribution).
- Unless it is clearly stated in the text of the publications, we assume that the quoted uncertainties on branching ratio and atomic mass dependence were taken into account in the systematic uncertainty. Thus for these terms, in the update of the uncertainties (quoted in Table 2), we subtract the original related to these two terms and we add in quadrature the latest ones.
- The results obtained by the CERN-PS experiment [21] using three different targets (H, C, W) have been fitted using $\alpha = 0.96 \pm 0.01$.
- As suggested in Ref. [34], we combine the results of NA51 [33] (H, D targets) and NA38 [34] (C, Al, Cu, W targets). In order to obtain total cross sections, the correction factors discussed in the NA51 paper are applied.
- The results of NA50 [35] on Be, Al, Cu, Ag and W targets are subject to a common fit of the A-dependence applying the correction factors discussed in the NA51 paper [33].
- The results of HERA-B [41] is a fit of the measurements obtained with C, Ti and W targets

The updated results for mid-rapidity and total cross sections are displayed in Fig. 1.

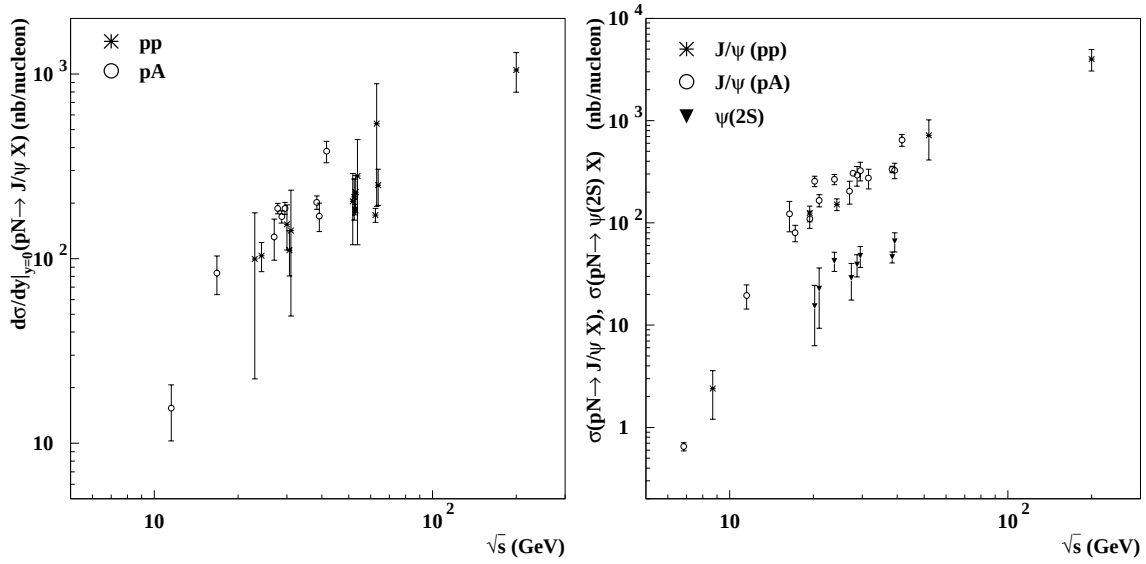

Figure 1: Production cross sections in proton-induced interactions from Table 2 as a function of the cms-energy. pp and pA measurements are indicated by different symbols. Left: Differential cross section $d\sigma_{pN}/dy$ at y=0; right: total cross section of J/ψ and $\psi(2S)$ production.

Experiment	Reaction	$\sqrt{s}$ (GeV)	$\frac{d\sigma_{J/\psi}}{dy}\|_{y=0}$ (nb/nucleon)	$\sigma_{J/\psi}$ (nb/nucleon)
CERN-PS [21]	pA	6.8		0.65 ± 0.06
WA39 [22]	pp	8.7		2.4 ± 1.2
IHEP [23]	pBe	11.5	16 ± 5.2	20 ± 5.2
E331 [24]	pBe	16.8	84 ± 20	122 ± 40
NA3 [25]	pPt	16.8		80 ± 15
NA3 [25]	pPt	19.4		110 ± 21
NA3 [25]	pp	19.4		124 ± 22
E331 [26]	pC	20.6		256 ± 30
E444 [27]	pC	20.6		166 ± 23
ISR [28]	pp	23.0	100 ± 77	
E705 [29]	pLi	23.8		267 ± 30
UA6 [30]	pp	24.3	104 ± 19	152 ± 20
E288 [31]	pBe	27.4	131 ± 33	204 ± 51
E595 [32]	pFe	27.4	187 ± 12	306 ± 18
NA38/51 [33, 34]	pA	29.1	169 ± 13	292 ± 64
NA50 [35]	pA	29.1	188 ± 14	325 ± 67
ISR [36]	pp	30	154 ± 42	
ISR [37]	pp	30.6	111 ± 30	
ISR [28]	pp	31	142 ± 93	
E672/706 [38]	pBe	31.6		274 ± 60
E771 [39]	pSi	38.8	202 ± 17	333 ± 25
E789 [40]	pAu	38.8	170 ± 30	327 ± 56
HERA-B [41]	pA	41.6	391 ± 51	663 ± 87
ISR [42]	pp	52	204 ± 85	716 ± 303
ISR [43]	pp	52	216 ± 54	
ISR [37]	pp	52.4	185 ± 12	
ISR [36]	pp	53	229 ± 52	
ISR [28]	pp	53	280 ± 161	
ISR [37]	pp	62.7	172 ± 15	
ISR [28]	pp	63	538 ± 346	
ISR [36]	pp	63	250 ± 56	
PHENIX [44]	pp	200	1051± 255	4000 ± 938

Table 2: Rescaled and updated differential ($d\sigma_{J/\psi}/dy$ at y=0) and total ($\sigma_{J/\psi}$) production cross sections in proton-induced interactions. The pA symbol in the second column indicate that the cross section value is obtained by fitting different target materials.

3.2 Compilation of $\psi(2S)$ cross sections

The procedure described in the previous section is applied to the published $\psi(2S)$ cross sections using the following parameters:

- The actual branching fractions [19] ($0.73 \pm 0.08\%$ for $\psi(2S) \to \mu^+\mu^-$ and $0.755 \pm 0.031\%$ for $\psi(2S) \to e^+e^-$) are applied.
- The target mass dependence is accounted for assuming $\alpha = 0.934 \pm 0.010$ [20] at $x_F(\psi(2S)) = 0$.

As a result, we obtain in Table 3 the absolute $\psi(2S)$ cross sections (see Fig. 1) and the ratio between J/ψ and $\psi(2S)$ cross sections (see Fig. 2). The last column of Table 3 indicates which one of these two quantities was directly measured by the experiments and has been used in the fit.

Experiment	Reaction	$\sqrt{s}$ (GeV)	$\sigma_{\psi(2S)}$ (nb/nucleon)	$\sigma_{\psi(2S)}/\sigma_{J/\psi}$ (R_ψ)	Quantity used in the fits
E331 [26]	pC	20.6	15.4 ± 9.1	0.060 ± 0.035	R_ψ
E444 [27]	pC	20.6	22.8 ± 13.5	0.137 ± 0.079	R_ψ
E705 [29]	pLi	23.8	42.5 ± 9.0	0.159 ± 0.029	R_ψ
E288 [31]	pBe	27.4	28.9 ± 11.3	0.141 ± 0.042	R_ψ
NA38/51 [33, 34]	pA	29.1	39.3 ± 9.6	0.135 ± 0.015	R_ψ
NA50 [35]	pA	29.1	47.1 ± 10.9	0.145 ± 0.017	$\sigma_{\psi(2S)}$
E771 [39]	pSi	38.8	46.3 ± 5.7	0.139 ± 0.020	$\sigma_{\psi(2S)}$
E789 [40]	pAu	38.8	66.1 ± 14.1	0.202 ± 0.055	$\sigma_{\psi(2S)}$

Table 3: Rescaled and updated total production cross sections of $\psi(2S)$ mesons and ratios of $\psi(2S)$ and J/ψ cross sections in proton-induced interactions.

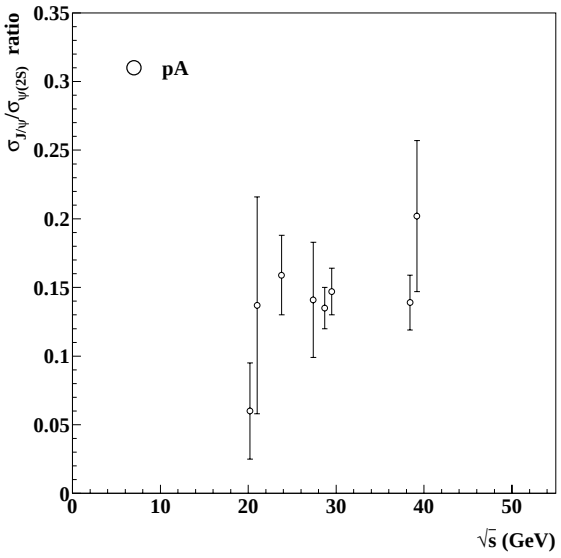

Figure 2: Ratio of J/ψ and $\psi(2S)$ cross section from Table 3 as a function of the cms-energy.

3.3 Comments on the available data

The J/ψ cross sections have been measured usually on large samples by triggering on dilepton decays. Therefore the most precise data have uncertainties dominated by systematic errors. The measurements show a good overall consistency, even though some of the results are hardly compatible. For instance, the two results at 20.6 GeV (E331 [26] and E444 [27]) differ by roughly 2σ. The E705 [29] result at 23.8 GeV exceeds the UA6 [30] one at 24.3 GeV by more than three σ, in contrast with the expectation that the cross section should increase with the cms-energy. This is a clear indication that some of the measurements have underestimated the systematic uncertainties coming from triggering effects or luminosity determination. Another approach has been followed by the HERA-B experiment [41] in analyzing a Minimum Bias data sample. In this case a small J/ψ statistics has been reconstructed, but the systematic uncertainites have been minimized.

The $\psi(2S)$ cross sections are estimated usually on the same data sample of the $\sigma_{J/\psi}$ but are poorer in statistics (by a factor around 60). Therefore they are less sensitive on the accurate determination of the systematic effects. Within the quoted uncertainties, there is a good internal consistency among the different measurements.

In the R_ψ cross section ratios, the systematic effects on luminosity or trigger mainly cancel out and the final uncertainty is usually dominated by the $\psi(2S)$ statistics. The measurements are all compatible.

4 Fit results

The cross sections values obtained from NRQCD calculations (see Eqs. 1, 3) have been used to fit the experimental results summarized in Tables 2, 3.

The ratio of the two octet matrix elements for J/ψ ($\lambda_{J/\psi}$) and $\psi(2S)$ ($\lambda_{\psi(2S)}$) production to the Tevatron ones are used to fit the theoretical predictions to the experimental values, by providing a kind of overall normalization.

Since the cross section depends on the product of the matrix elements and the PDF's as shown in Eq. 1, a change of the PDF can influence the result of the fit on the two octet matrix elements. For these reasons two different PDF functions have been used in the fit procedure. The PDF used are the most recent ones, namely the CTEQ6m [16] and the MRST2002nlo [17].

The data considered in the fit include 21 results on the total J/ψ cross section in a cms-energy range between 6.7 and 200 GeV, 3 $\psi(2S)$ cross sections (cms-energy range: [29.1:38.8] GeV) and 5 cross section ratios $R_\psi = \sigma_{\psi(2S)}/\sigma_{J/\psi}$ (cms-energy range: [20.6:38.8] GeV), for a total of 29 experimental results.

This set of data shows a good overall consistency, except for the few measurements on $\sigma_{J/\psi}$ already mentioned in the previous chapter.

As a first step, the fit has been performed on all the 29 experimental results by exploiting the MRST2002nlo and the CTEQ6m PDFs. Since the charmonium production from singlet states depends strongly on the factorization and renormalization scale used in the PDF, we have decided to choose the proper scale following an optimization procedure. As a matter of fact we have fitted the data with different scale factors and we have chosen for each PDF the value that provided the smallest χ^2. The optimal scale values obtained with this procedure are $\mu = 1.5\mu_0$ for MRST2002nlo and $\mu = 2.6\mu_0$ where $\mu_0 = 2m_c$. The fit results obtained with these scale values are reported in Table 4.

The χ^2 of the fit is poor for both fits, since, as previously discussed, the measurements are not all internally compatible. A reasonable explanation is that in some cases the experimental uncertainty might have been underestimated. With this assumption, we increased the uncertainties of the fit results

	MRST2002nlo	CTEQ6m
μ	$1.5\mu_0$	$2.6\mu_0$
χ^2/dof	114/27	171/27
Uncertainty scale (s)	2.05	2.51
$\lambda_{J/\psi}$	0.090 ± 0.019	0.211 ± 0.035
$\lambda_{\psi(2S)}$	0.061 ± 0.013	0.112 ± 0.023
$\sigma_{J/\psi}$ (nb/nucleon)	502 ± 32	522 ± 41
$\sigma_{\psi(2S)}$ (nb/nucleon)	65 ± 9	65 ± 11
$R_\psi = \sigma_{\psi(2S)}/\sigma_{J/\psi}$	0.130 ± 0.018	0.125 ± 0.021

Table 4: Results of the fit performed using the optimal scale factors for the MRST2002nlo and the CTEQ6m PDFs. The cross sections and the ratio R_ψ are quoted for the HERA-B cms-energy ($\sqrt{s} = 41.6\ GeV$).

by a scaling factor s (third row of Table 4) adopting the PDG prescription ([19]). The ratios of the matrix elements ($\lambda_{J/\psi}$, $\lambda_{\psi(2S)}$) provided by the fits differ by about a factor two mainly because of the different scale factors used.

Nevertheless, in both fits the color octet matrix elements are found to be much smaller ($10\% - 20\%$) than those extracted at the Tevatron. The results on the J/ψ and $\psi(2S)$ cross sections as well as on the ratio R_ψ at the HERA-B cms-energy are instead quite insensitive to the PDF choices, whose dependence is almost completely reabsorbed in the λ's (see lower section of Table 4). Given that the CTEQ6m PDF shows a worse adaptation to the data, we have decided to choose the MRST2002nlo PDF fit (with $\mu = 1.5\mu_0$) as our baseline fit, while the results from the CTEQ6m PDF ($\mu = 2.6\mu_0$) have been considered in the systematic uncertainties determination.

The fit results as a function of the cms-energy are displayed in Fig. 3. In the left plot the J/ψ cross section is shown. In the central plot the $\psi(2S)$ cross section is shown, while the $\sigma_{\psi(2S)}/\sigma_{J/\psi}$ ratio is displayed in the right plot. The open circles in the central and right plots represent the results calculated from the published papers and not used in the fit (see Table 3). The dot-dashed line indicates the NRQCD predictions without any octet contribution in the charmonium production, while the continuous line is the result of the fit (which determines the two octet matrix elements). Finally the two dotted lines are referring to the uncertainties of the fit.

The stability of the results with respect to our baseline fit and the systematic uncertainties have been checked with detailed studies. On one side we have varied the fit conditions by changing the selection of the measurements or the PDF. On the other side we have determined the systematic uncertainty due to the PDF by following the prescriptions of the PDF groups [45].

In the following we list the different fit strategies. The corresponding results are shown Table 5.

- The fit was performed by excluding all the experimental results which show a bad partial χ^2 (χ^2_p) and consequently are not compatible with the NRQCD calculations (see row 2 of Table 5). We then decided to exclude all the measurement with $\chi^2_p > 9$ (corresponding to a 3σ discrepancy). As a result the four results on J/ψ cross section from the E331 [26], E705 [29], E595 [32] and E771 [39] experiments were excluded and we obtained a new result with a much improved χ^2 ($\chi^2/dof = 37/23$) .

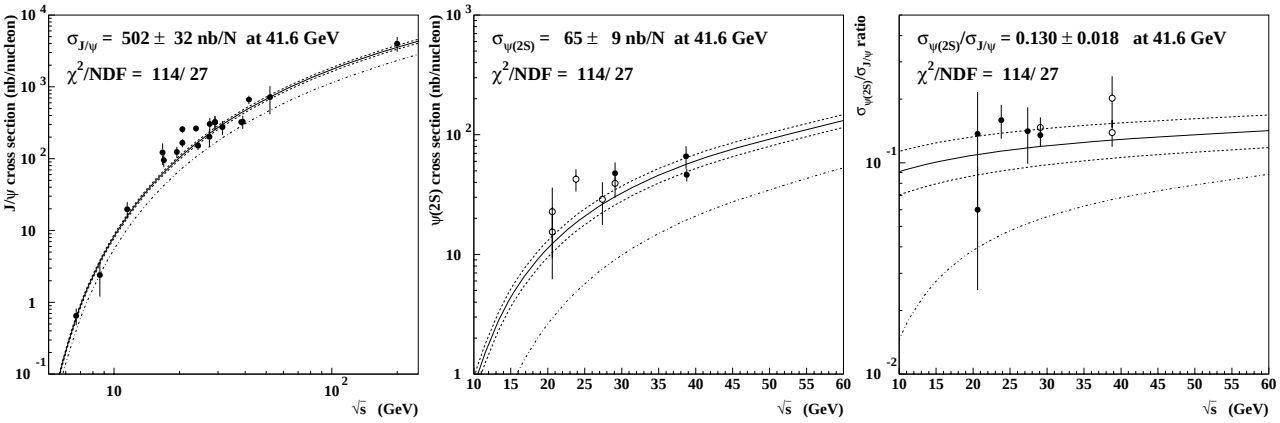

Figure 3: Fit results as a function of the cms-energy for the J/ψ cross section (left), the $\psi(2S)$ cross section (center) and the $\sigma_{\psi(2S)}/\sigma_{J/\psi}$ ratio (right). The open circles in the central and right plots represent the results calculated from the published papers and not used in the fit.

	χ^2/dof	$\sigma_{J/\psi}$ (nb/nucleon)	$\sigma_{\psi(2S)}$ (nb/nucleon)	$\sigma_{\psi(2S)}/\sigma_{J/\psi}$	Comments
1	114/27	502 ± 32	65 ± 9	0.130 ± 0.018	All the data
2	37/23	491 ± 27	65 ± 5	0.132 ± 0.012	As *1* without $\chi^2 > 9$ measurements
3	109/21	511 ± 37	66 ± 9	0.129 ± 0.019	As *1* with $\sqrt{s} \in [19 : 63]$ GeV
4	54/16	549 ± 46	77 ± 20	0.140 ± 0.035	As *1* with $A < 14$
5	114/25	500 ± 33	65 ± 9	0.130 ± 0.018	As *1* without collider experiments
6	37/27	487 ± 29	65 ± 4	0.133 ± 0.011	As *1* with all the uncertainties on J/ψ cross sections x2
7	70/23	479 ± 29	64 ± 7	0.134 ± 0.016	As *1* without incompatible measurements
8	127/27	497 ± 33	59 ± 6	0.119 ± 0.013	As *1* with the errors on J/ψ and $\psi(2S)$ BR's put to zero
9	171/27	522 ± 41	65 ± 11	0.125 ± 0.021	As *1* with the CTEQ6m PDF

Table 5: Results of the fit performed using the MRST2002nlo PDF (row 1 - 8) and CTEQ6m (row 9). The cross section values are calculated at the HERA-B cms-energy ($\sqrt{s} = 41.6$ GeV).

- The fit was applied only to the measurements performed in a cms-energy range between 14 and 63 GeV in order to check the influence of the low-energy and high-energy points on the fit results (see row 3 of Table 5).

- The fit was applied only to the proton-proton or proton-nucleus measurements with atomic weight (A) less than 14 in order to minimize the possible effect of the A-dependence (see row 4 of Table 5).
- The fit was applied only to the proton-nucleus fixed target measurements excluding the collider experiment (see row 5 of Table 5).
- All the experimental uncertainties on the J/ψ cross sections were arbitrary enlarged by a factor two, in order to decrease the total χ^2 without excluding any experiment (see row 6 of Table 5).
- The fit was applied excluding the four incompatible measurements on $\sigma_{J/\psi}$ at 20.6, 23.8 and 24.3 GeV (E331 [26], E444 [27], E705 [29] and UA6 [30]) as discussed in the text (see row 7 of Table 5).
- All the experimental uncertainties on the J/ψ and $\psi(2S)$ branching ratios were arbitrary set to zero in order to check the effect of the correlations between the uncertainties of the experimental results (see row 8 of Table 5).

As one can see, the fit results are quite stable showing a maximal variation smaller than 10% with respect to the baseline solution.

The same list of fits was then applied to the data by using the CTEQ6m PDF ($\mu = 2.6\mu_0$). The fits provide for all the cases a larger χ^2, while the results on the cross sections are compatible with the MRST2002nlo ones ($\mu = 1.5\mu_0$). In Fig. 4 the fit results on the J/ψ cross section as a function of the cms-energy are shown for the baseline data selection for the MRST2002nlo and for the CTEQ6m PDFs. Although the overall energy-dependent behavior of the two curves is similar, the MRST2002nlo curve describes better the data and hence has a lower χ^2. Independently of the PDF used, the cross section results at the HERA-B energy are quite stable showing a variation on the total J/ψ cross section of less than 5% with respect to the baseline result independently on the PDF used. The results corresponding to the baseline fits with the MRST2002nlo and the CTEQ6m PDF are shown respectively in row 1 and 9 of Table 5.

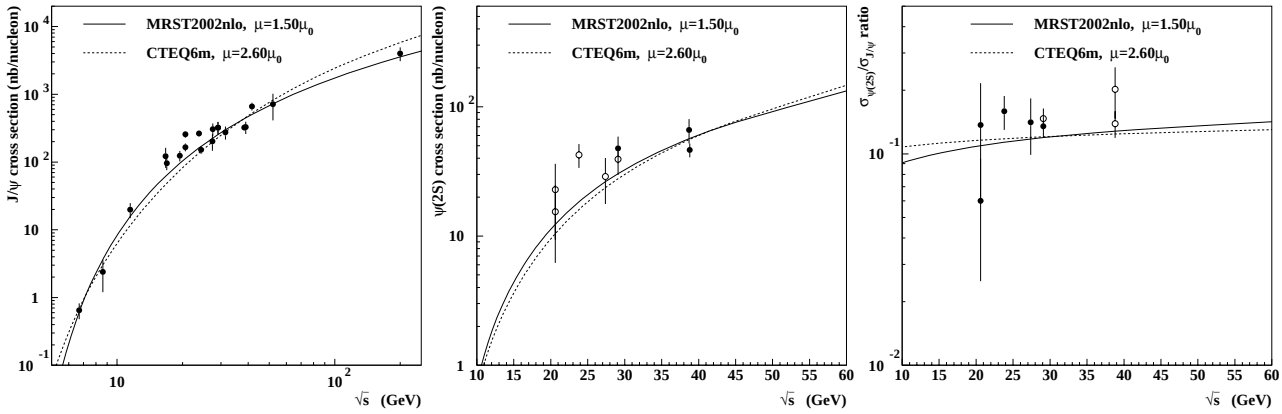

Figure 4: Fit results as a function of the cms-energy for the J/ψ, ψ' cross sections and their ratio. The continuous line corresponds to the MRST2002nlo PDF and the dashed line to the CTEQ6m PDF.

The systematic uncertainties related to the PDF have been calculated using the so called "Les Houches Accord" prescription [45]. The essence of this method consists in evaluating for each initial PDF set several derived PDFs each one grasping the uncertainty in one of PDF fit parameters. By calculating

the cross sections for each derived PDF it is possible to evaluate the systematic uncertainty related to a specific PDF. This calculation has been performed for the CTEQ6m PDF which has 40 derived PDFs associated to it and for the MRST2001 PDF which has 30 derived PDFs. At the moment it is not possible to perform the same analysis with the MRST2002nlo PDF, but we checked that the difference between the MRST2002nlo and the MRST2001 PDF is at the level of 1%. Therefore we estimate the systematic uncertainty on the MRST2002nlo based on the results of the MRST2001 PDF. For this PDF, there is a broad energy range 19-200 GeV where the systematic uncertainties on the J/ψ cross section are below 5% and tend to increase as lower energies are approached. Systematic uncertainties calculated with the CTEQ6m PDF are usually larger by a factor two, a well known fact which is related to the treatment of the incompatible data made by the two PDF groups. Although for some of the energies the systematic uncertainties are large, no systematic bias is present in our baseline solution. This can be seen, for example, in Table 5: in the fit nr. 3 only the energy region of best systematic uncertainty has been considered in the fit and the final result is very well consistent with the baseline solution.

	Fit uncertainty	Data selection	PDF uncertainty	Total uncertainty
$\Delta\sigma_{J/\psi}$ (nb/nucleon)	± 32	± 20	± 22	± 44
$\Delta\sigma_{\psi(2S)}$ (nb/nucleon)	± 9	± 5	± 2	± 11
ΔR_ψ ($\times 10^{-3}$)	± 18	± 6	± 2	± 19

Table 6: Main uncertainties in the J/ψ and $\psi(2S)$ cross sections and their ratio. The second column shows the scaled fit uncertainties; the third column contains the systematic uncertainty due to the data selection while the fourth contains the PDF uncertainty. In the last column there are the total uncertainties obtained by adding quadratically the previous errors.

In Table 6, all the uncertainties coming from the fits have been collected. We consider only three types of uncertainties: statistical, systematic from the data selection and systematic uncertainty from the PDF. The statistical uncertainties are evaluated from the fit. The actual fit result has been scaled to take into account the large χ^2. Since the J/ψ data are intrinsically inconsistent, the variation of the results with respect to the removal of problematic data points is considered a systematic uncertainty. The actual value we quote is obtained as the maximal variation range observed divided by $\sqrt{12}$. The second systematic uncertainty is the PDF uncertainty evaluated as discussed in [45]. Since these errors are uncorrelated, in the last column we quote the quadratic sum as our final uncertainty.

5 Conclusions

A detailed study based on NRQCD calculation has been performed in order to fit all the available experimental data on J/ψ and $\psi(2S)$ productions. Many fits have been performed by exploiting different measurements and different parton distribution functions (PDF).

The results at the HERA-B energy derived from the fit for the total J/ψ and $\psi(2S)$ cross sections are the following:

$$\sigma_{J/\psi} = (502 \pm 44) \text{ nb/nucleon} \tag{8}$$

$$\sigma_{\psi(2S)} = (65 \pm 11) \text{ nb/nucleon} \tag{9}$$

$$R_\psi = (0.130 \pm 0.019) \tag{10}$$

where the systematic uncertainties take into accounts the variation of the results in the different fits performed and the uncertainties due to the PDF.

References

[1] E. L. Berger and D. L. Jones, Phys. Rev. D **23** 1521 (1981).

[2] R. Baier and R. Ruckl, Phys. Lett. B **102**, 364 (1981).

[3] G. T. Bodwin, E. Braaten, and G. P. Lepage, Phys. Rev. D **51**, 1125 (1995) [Erratum-ibid. D **55**, 5853 (1997)].

[4] M. Krämer, Prog. Part. Nucl. Phys. **47**, 141 (2001).

[5] CDF collaboration, Note 05-04-28.

[6] M. Beneke and M. Krämer, Phys. Rev. D **55**, 5269 (1997).

[7] G. P. Lepage, L. Magnea, C. Nakhleh, U. Magnea and K. Hornbostel, Phys. Rev. D **46**, 4052 (1992).

[8] G. C. Nayak, J. W. Qiu and G. Sterman, [hep-ph/0509021].

[9] F. Maltoni, M. L. Mangano and A. Petrelli, Nucl. Phys. B **519**, 361 (1998).

[10] A. Petrelli, M. Cacciari, M. Greco, F. Maltoni, and M. L. Mangano, Nucl. Phys. **B514**, 245 (1998).

[11] M. Kramer, Nucl. Phys. B **459**, 3 (1996).

[12] W. Buchmüller and S. H. Tye, Phys. Rev. **D24**, 132 (1981).

[13] E. J. Eichten and C. Quigg, Phys. Rev. **D52**, 1726 (1995).

[14] F. Abe et al., (CDF Collaboration), Phys. Rev. Lett. **79**, 572 (1997).

[15] P. Nason *et al.*, [hep-ph/0003142].

[16] H.L. Lai et al., Eur. Phys. J.**12**, 375 (2000).

[17] A.D. Martin et al., Eur. Phys. J.**28**, 455 (2003).

[18] G. T. Bodwin, E. Braaten and J. Lee, Phys. Rev. D **72** (2005) 014004.

[19] S. Eidelmann et al., Review of Particle Physics, Phys. Lett. B **592**, 1 (2004).

[20] M.J. Leitch et al., (E866 collaboration), Phys. Rev. Lett. **84**, 3256 (2000).

[21] A. Bamberger et al., Nucl. Phys. B **134**, 1 (1978).

[22] M.J. Corden et al. (WA39 collaboration), Phys. Lett. **98B**, 220 (1981).

[23] Yu.M. Antipov et al., Phys. Lett. **60B**, 309 (1976).

[24] K.J. Anderson et al., Phys. Rev. Lett. **36**, 237 (1976), Phys. Rev. Lett. **37**, 799 (1976).

[25] J. Badier et al., (NA3 collaboration), Z. Phys. C **20**, 101 (1983).

[26] J.G. Branson et al., (E331 collaboration), Phys. Rev. Lett. **38**, 1331 (1977).

[27] K.J. Anderson et al., (E444 collaboration), Phys. Rev. Lett. **42**, 944 (1979).

[28] J.H. Cobb et al., Phys. Lett. **68B**, 101 (1977).

[29] L. Antoniazzi et al., (E705 collaboration), Phys. Rev. D **46**, 4828 (1992).

[30] C. Morel et al., (UA6 collaboration), Phys. Lett. B **252**, 505 (1990).

[31] H.D. Snyder et al., (E288 collaboration), Phys. Rev. Lett. **36**, 1415 (1976).

[32] E.J. Siskind et al., (E595 collaboration), Phys. Rev. D **21**, 628 (1980).

[33] M.C. Abreu et al., (NA51 collaboration), Phys. Lett. B **438**, 35 (1998).

[34] M.C. Abreu et al., (NA38 collaboration), Phys. Lett. B **444**, 516 (1998).

[35] B. Alessandro et al., (NA50 collaboration), Eur. Phys. J. C **33**, 31 (2004).

[36] C. Kourkoumelis et al., Phys. Lett. **91B**, 481 (1980).

[37] A.G. Clark et al., Nucl. Phys. B **142**, 29 (1978).

[38] A. Gribushin et al., (E672/706 collaboration), Phys. Rev. D **62**, 012001 (2000).

[39] T. Alexopoulos et al., (E771 collaboration), Phys. Rev. D **55**, 3927 (1997).

[40] M.H. Schub et al., (E789 collaboration), Phys. Rev. D **52**, 1307 (1995).

[41] I. Abt et al., (HERA-B collaboration), DESY Report 05-232, submitted to Phys. Lett. B.

[42] E. Nagy et al., Phys. Lett. **60B**, 96 (1975).

[43] E. Amaldi et al., Lett. Nuo. Cim. **19**, 152 (1977).

[44] S.S. Adler et al., (PHENIX collaboration), Phys. Rev. Lett. **92**, 051802 (2004).

[45] J. Pumplin et al., JHEP **0207**, 012 (2002).